

Marquette University

e-Publications@Marquette

Chemistry Faculty Research and Publications

Chemistry, Department of

4-1999

Visible and Resonance Raman Spectra of Low Valent Iron Porphyrins

Chathra De Silva
Marquette University

Kazimierz Czarnecki
Marquette University

Michael D. Ryan
Marquette University, michael.ryan@marquette.edu

Follow this and additional works at: https://epublications.marquette.edu/chem_fac

 Part of the [Chemistry Commons](#)

Recommended Citation

Silva, Chathra De; Czarnecki, Kazimierz; and Ryan, Michael D., "Visible and Resonance Raman Spectra of Low Valent Iron Porphyrins" (1999). *Chemistry Faculty Research and Publications*. 431.
https://epublications.marquette.edu/chem_fac/431

Marquette University

e-Publications@Marquette

Department of Chemistry Faculty Research and Publications/College of Arts and Sciences

This paper is NOT THE PUBLISHED VERSION; but the author's final, peer-reviewed manuscript. The published version may be accessed by following the link in the citation below.

Inorganica Chimica Acta, Vol. 287, No. 1 (April 2, 1999): 21-26. [DOI](#). This article is © Elsevier and permission has been granted for this version to appear in [e-Publications@Marquette](#). Elsevier does not grant permission for this article to be further copied/distributed or hosted elsewhere without the express permission from Elsevier.

Visible and Resonance Raman Spectra of Low Valent Iron Porphyrins

Chathra De Silva

Department of Chemistry, Marquette University, Milwaukee, WI

Kazimierz Czarnecki

Department of Chemistry, Marquette University, Milwaukee, WI

Michael D Ryan

Department of Chemistry, Marquette University, Milwaukee, WI

Abstract

The [resonance Raman spectrum](#) of $\text{Fe}(\text{TPP})^{2-}$ was obtained after the three-electron [electrochemical reduction](#) of $\text{Fe}(\text{TPP})(\text{Cl})$. The coulometric reduction was carried out in the presence of bis(triphenylphosphoanylidine)ammonium chloride in DMF in order to avoid the formation of iron- σ -alkyl complexes. The resonance Raman spectrum of the intermediate [oxidation](#) states ($\text{Fe}(\text{TPP})$ and $\text{Fe}(\text{TPP})^-$) were

consistent with previous work. The spectrum of the three-electron product, $\text{Fe}(\text{TPP})^{2-}$, obtained at 442 nm, was qualitatively similar to the two-electron reduced product, $\text{Fe}(\text{TPP})^-$, with an intense ν_2 band at 1537 cm^{-1} . The high frequency bands generally decreased in energy, contrary to the expectations based on the X-ray crystallographic core size. In particular, the ν_2 and ν_{10} bands decreased by 18 and 22 cm^{-1} . A small increase was observed for the ν_4 band ($+4\text{ cm}^{-1}$). While these changes were not consistent with the measured core size, they were in agreement with other [porphyrin](#) π -anion radicals such as $\text{Zn}(\text{TPP})^-$ and $\text{VO}(\text{OEP})^-$. Based on the resonance Raman spectra, $\text{Fe}(\text{TPP})^{2-}$ can be formulated as an iron(I) π -radical anion. Significant backbonding between the d_{π} -orbitals of the iron to the e_g^* orbital of the porphyrin, though, is probably occurring. As a result, the complex is probably not a pure π -anion radical.

Keywords

Iron complexes, Porphyrin complexes, Low valent complexes

1. Introduction

The electronic structure of low valent metalloporphyrins has been the subject of considerable studies over the past several years. When an electron is added to a four-coordinate iron(II) porphyrin, the electron may either reduce the iron(II) to iron(I) or the porphyrin to the π -anion (or some combination). Addition of a second electron leads to additional possibilities (iron(0), iron(I)- π -anion, iron(II)-dianion). $\text{Fe}(\text{P})^-$ and $\text{Fe}(\text{P})^{2-}$ porphyrins have been investigated by a variety of spectroscopic techniques including UV-Vis [\[1\]](#), [\[2\]](#), [\[3\]](#), Mössbauer [\[1\]](#), resonance Raman [\[4\]](#), [\[5\]](#), [\[6\]](#), proton [\[2\]](#), [\[7\]](#) and deuterium [\[8\]](#) NMR spectroscopy. X-ray structures of $\text{Fe}(\text{TPP})^-$ and $\text{Fe}(\text{TPP})^{2-}$ have also been reported [\[3\]](#).

The electronic structures of these complexes are still controversial. Mashiko et al. [\[3\]](#) characterized $\text{Fe}(\text{TPP})^-$ as a resonance hybrid of a d^7 iron(I) porphyrin and an $S=1$ d^6 iron(II) π -radical anion. On the other hand, Hickman et al. [\[8\]](#) assigned the structure of $\text{Fe}(\text{TPP})^-$ as an iron(I) porphyrin, with the unpaired electron density in a σ -based molecular orbital (d_z^2), based on ^2H NMR. Sinyakov and Shulga [\[2\]](#) also favored an iron(I) porphyrin, but with a $(d_{xy})^2(d_{xz}, d_{yz})^3(d_z^2)^2$ formulation. Donohoe et al. [\[4\]](#), using resonance Raman spectroscopy, supported the low spin iron(I) structure, with significant backbonding from the iron to the porphyrin. Teraoka et al. [\[5\]](#), though, favored a high-spin d^7 complex for $\text{Fe}(\text{OEP})^-$, while Yamaguchi and Morishima [\[7\]](#) provided NMR and EPR evidence for a low-spin d^7 structure of the same complex.

The structure of the complex was highly dependent upon the electron withdrawing nature of the porphyrin macrocycle. Yamaguchi and Morishima [\[7\]](#) investigated the proton NMR spectra of β -pyrrole substituted porphyrins and were able to change the electronic structure from an iron(I) porphyrin to an iron(II) π -anion radical. Donohoe et al. [\[4\]](#) had observed earlier the same transitions with tetraphenylporphyrins, using resonance Raman spectroscopy. The resonance Raman spectra of several complexes that are clearly π -anion radicals, such as the one electron reduced $\text{Zn}(\text{P})$ [\[6\]](#), [\[9\]](#), [\[10\]](#), [\[11\]](#), [\[12\]](#) and $\text{VO}(\text{P})$ [\[12\]](#), have been studied to provide markers for the π -anion radical species.

There is perhaps more uncertainty on the structure of $\text{Fe}(\text{P})^{2-}$ complexes. Mashiko et al. [\[3\]](#) found no compelling evidence for an iron(0) contribution to the structure, and favored a $\text{Fe}^1(\text{TPP})^{2-}$ (iron(I) π -radical anion) structure. Hickman et al. [\[8\]](#) also favored an iron(I) π -radical anion structure, based on deuterium NMR. On the other hand, Sinyakov and Shulga [\[2\]](#) tentatively interpreted the proton NMR spectra as an iron(0) porphyrin, with significant backbonding from the metal. Anxolabéhère et al. [\[6\]](#) also supported an iron(0) structure, based on resonance

Raman spectra. Their reported spectra, though, differed in many respects from results that were being obtained in our laboratory. The origin of these differences was investigated in detail and form the basis of this report.

2. Experimental

2.1. Chemicals

Iron(III) tetraphenylporphyrin chloride (chlorin-free) was purchased from MidCentury Chemicals and was used as received. *N,N*-Dimethylformamide (DMF, anhydrous) was obtained from Aldrich and was purified by heating over calcium hydride and then distillation under reduced pressure. Care was taken to avoid exposure to the atmosphere by flushing the receiving container with argon gas. Bis(triphenylphosphoanylidine)ammonium chloride (PNPCI) was obtained from Aldrich. Tetrabutylammonium (TBAP) and tetraethylammonium (TEAP) perchlorate were obtained from GFS Chemical. The salts (PNPCI, TBAP and TEAP) were dried under vacuum at 70°C for several hours. Tetrabutylammonium hydroxide (1.0 M) was obtained from Aldrich. Solutions of $\text{Fe}^{\text{II}}(\text{TPP})(\text{OH})^-$ were obtained by electrolysis of $\text{Fe}(\text{TPP})(\text{Cl})$ to $\text{Fe}(\text{TPP})$, followed by addition of an appropriate amount of tetrabutylammonium hydroxide. The formation of the complex was assured by visible spectroscopy, and the solutions were kept under strict anaerobic conditions.

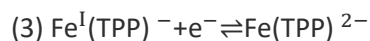
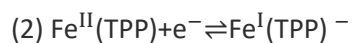
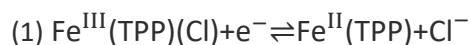
2.2. Equipment

An optically transparent thin layer electrochemical cell (OTTLE) [13] was used for the visible spectroelectrochemistry experiments. The visible spectra were recorded on a Hewlett–Packard 8452A diode array spectrophotometer. Low-temperature spectroelectrochemistry (OTTLE) was carried out by passing cooled dinitrogen over the face of the OTTLE cell. The sample for resonance Raman spectroscopy was obtained by electrolysis in a three-electrode coulometric cell [14], consisting of a platinum gauze working electrode, a platinum wire auxiliary electrode and an $\text{Ag}/0.1 \text{ M AgNO}_3$ reference electrode (in acetonitrile). The reference electrode was separated from the electrolysis solution by a Vycor tipped salt bridge, filled with the same electrolyte as the electrolysis solution. The auxiliary electrode was separated from the electrolysis solution with a Vycor tubing salt bridge. Argon was used to purge air from the electrolysis solution, and controlled potential electrolysis was performed with an Electrosynthesis model 410 potentiostat with an EG&G PARC model 379 digital coulometer. Resonance Raman spectra were obtained with an He–Cd laser (Liconix 4240NB) with 442 nm excitation with a 1269 SPEX single monochromator equipped with a charge coupled detector (CCD). Low laser power was applied to the sample solution by using a cylindrical lens. Spectra were recorded at room temperature.

3. Results

3.1. Spectroelectrochemical studies

Three reduction waves can be observed in the electrochemistry of $\text{Fe}(\text{TPP})(\text{Cl})$:



Under anaerobic conditions, $\text{Fe}(\text{TPP})$ and $\text{Fe}(\text{TPP})^-$ are quite stable, but $\text{Fe}(\text{TPP})^{2-}$ forms iron–alkyl complexes [15] in the presence of the tetraalkylammonium salts, that are generally used as the supporting electrolyte in electrochemical studies. Before pursuing the resonance Raman spectroscopy of these electrochemically

generated species, spectroelectrochemical studies were initiated in order to find the conditions that $\text{Fe}(\text{TPP})^{2-}$ would be stable. The long term stability of the low-valent species was monitored using a thin layer spectroelectrochemical cell. A slow cyclic potential scan ($\approx 1 \text{ mV s}^{-1}$) was initiated, and the absorbance was monitored at a particular wavelength (e.g. 414 nm, in the Soret region). This technique is called cyclic voltabsorptometry (CVA) [16].

The CVA for $\text{Fe}(\text{TPP})(\text{Cl})$ in DMF with TBAP or PNPCI as the supporting electrolyte is shown in Fig. 1. The decrease in absorbance between -0.6 and -0.9 V was due to the reduction of $\text{Fe}(\text{TPP})(\text{Cl})$ to $\text{Fe}(\text{TPP})$ (reaction 1). As the potential was scanned more negative, the absorbance decreased further in two waves due to the formation of $\text{Fe}(\text{TPP})^-$ (reaction 2) and $\text{Fe}(\text{TPP})^{2-}$ (reaction 3). For curve A (TEAP), the absorbance change on the reverse scan did not reverse the absorbance changes of the forward scan. In particular, the absorbance of $\text{Fe}(\text{TPP})^{2-}$ was not stable, and the re-oxidation of $\text{Fe}(\text{TPP})^{2-}$ did not return to the original $\text{Fe}(\text{TPP})^-$ absorbance value. In addition, a new wave (due to the alkyl complex) was observed at about -1.2 V . When PNPCI was used as the supporting electrolyte (curve B), $\text{Fe}(\text{TPP})^-$ and $\text{Fe}(\text{TPP})$ can be completely regenerated. In the presence of the high concentrations of chloride ion, the ferrous complex exists mostly as the chloro complex, and the wave was shifted to more negative potentials [17]:

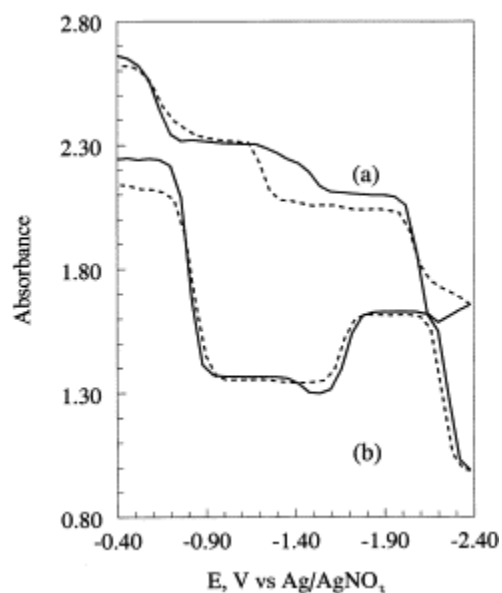
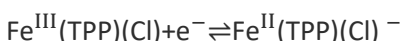


Fig. 1. Absorbance at 414 nm as a function of potential (CVA scan) during a 1 mV s^{-1} cyclic scan. 1.0 mM $\text{Fe}(\text{TPP})(\text{Cl})$ in DMF. (a) 0.10 M TBAP. (b) 0.10 M PNPCI. Forward scan: solid line; reverse scan: dashed line. Temperature: 23°C .

The $\text{Fe}(\text{TPP})^{2-}$ is unstable not just in the presence of the tetrabutylammonium ion, but also in the presence of other alkyl ammonium salts. The reaction of $\text{Fe}(\text{TPP})^{2-}$ with the tetraethylammonium ion can be observed in Fig. 2. The spectrum of $\text{Fe}(\text{TPP})^{2-}$ was initially formed at -2.2 V during a linear scan at 1 mV s^{-1} . As the scan continues, the formation of the alkyl complex can be observed with the Soret band around 435 nm . Using ^2H NMR, it was shown that the tetraalkylammonium salt was the source of the alkyl ligand, rather than the solvent itself [18]. As a result, the long term stability of $\text{Fe}(\text{TPP})^{2-}$ at room temperature could only be assured with salts such as PNPCI in DMF, the solvent/electrolyte system that was used in this work for obtaining the resonance Raman spectra.

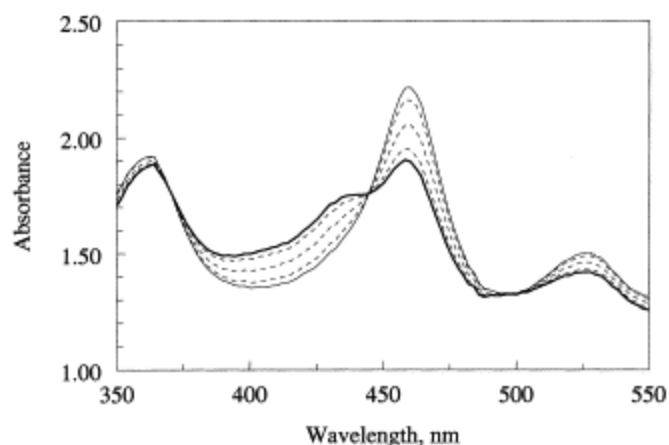


Fig. 2. Spectral changes of Fe(TPP)(Cl) while scanning through the third wave at 1 mV s^{-1} . The solid line spectrum is Fe(TPP)^{2-} , the bold line spectrum is the final spectrum of the scan, and the dashed lines are intermediate spectra taken in 2 min intervals. Solvent: DMF; electrolyte: 0.10 M TEAP; temperature: 23°C .

The visible spectra for Fe(TPP) , Fe(TPP)(Cl)^- , Fe(TPP)^- and Fe(TPP)^{2-} , obtained using CVA, were consistent with previously reported values [6], [15], [19], [20]. Unfortunately, PNPCL is not soluble in THF, and TBAP must be used instead. As a result, all the resonance Raman spectra were obtained using DMF. At about 4°C , the alkylation reaction in THF was slow enough so that the spectrum of Fe(TPP)^{2-} could be determined. Under these conditions, a spectrum almost identical to the complex in DMF was observed, with Soret bands at 360 and 460 nm. When sodium metal was used as a reductant, the Soret bands in THF appeared at 358 and 448 nm [3], [21]. Because of the presence of trace water in the alkali perchlorate salts, it was not possible to generate Fe(TPP)^{2-} electrochemically in the presence of sodium or lithium ions. These spectral differences are probably due to ion-pairing.

3.2. Resonance Raman spectroscopy

The resonance Raman spectra of Fe(TPP)Cl at various degrees of reduction in DMF are shown in Fig. 3 and Table 1. At -1.3 V , the spectrum for Fe(TPP)(Cl)^- was observed. The resonance Raman spectrum, which was obtained using 442 nm laser excitation, was quite strong because the Soret band for this species occurs at 440 nm. The resonance Raman spectrum was quite similar to other high-spin five-coordinate ferrous porphyrin complexes such as Fe(TPP)(OH)^- (Table 1).

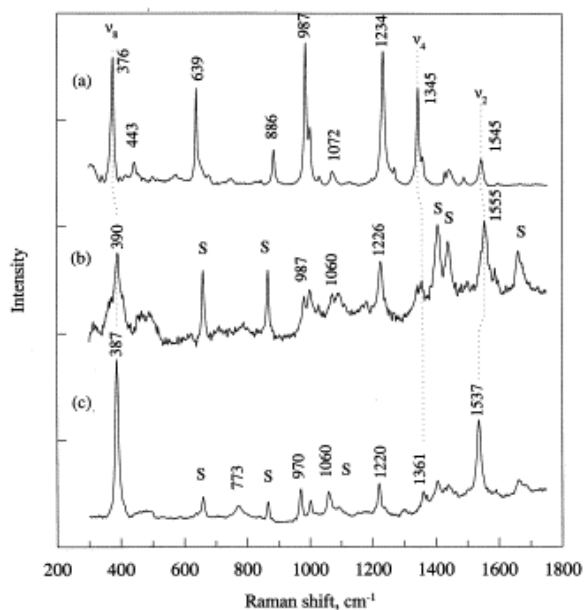


Fig. 3. [Resonance Raman spectra](#) of 1.0 mM Fe(TPP)(Cl) in DMF with 0.1 M PNPCI at: (a) -1.3 V ($\text{Fe}^{\text{I}}(\text{TPP})$); (b) -1.8 V ($\text{Fe}(\text{TPP})^-$); and (c) -2.3 V ($\text{Fe}(\text{TPP})^{2-}$) vs. 0.1 M Ag/AgNO₃. Laser power: 28 mW, excitation wavelength: 442 nm.

Table 1. [Resonance Raman spectra](#) of iron [porphyrin](#) complexes

Mode	Fe(TPP)(Cl)-	Fe(TPP) ^{-a}	Fe(TPP) ²⁻	Fe(TPP)(OH)-
ν_{10}	1597	1563	1540 (dp)	1600
ν_2	1545	1555 (1555)	1537 (p, 0.34)	1545
ν_{11}	1491		1465 (dp, 0.77)	
ν_3	1443		1426 (p, 0.27)	1441
			1372 (dp)	
ν_4	1345	1357 (1356)	1361 (p, 0.11)	1341
			1349 (ap)	
			1304 (p)	
ν_1	1234	1226 (1224)	1220 (p, 0.14)	1233
			1207 (ap)	
ν_9	1072	1060	1060 (p)	1076
φ_7	1031	1029		1031
ν_6	1002	1002	1002 (0.46)	1002
φ_8	986	987	970 (p)	985
ν_7	885		878 (p)	885
ν_{16}	845		842 (dp)	845
			772 (p)	
π_3	680			
φ_9	638		639 (p)	638
	443			442
ν_8	375	389	387 (p)	372

^aRef. [4] in parentheses.

Further reduction at -1.8 V gave rise to the $\text{Fe}(\text{TPP})^-$ spectrum. Great care must be taken in assuring complete reduction of the iron–porphyrin complex because iron(I) bands are much weaker than the iron(II) bands. The spectrum for $\text{Fe}(\text{TPP})^-$ agreed quite well with the values obtained by Donohoe et al. [4] (Table 1). The intensity of the solvent bands in curve (b) of Fig. 3 demonstrates the relative weakness of the $\text{Fe}(\text{TPP})^-$ resonance Raman spectra compared with $\text{Fe}(\text{TPP})(\text{Cl})^-$. Except for ν_4 and ν_8 , the bands generally shifted to lower energy upon reduction.

At -2.3 V, the resonance Raman spectrum of $\text{Fe}(\text{TPP})^{2-}$ could be obtained (Table 1). The spectrum was qualitatively similar to $\text{Fe}(\text{TPP})^-$, but the bands were generally more intense and shifted to lower energies. For example, the ν_2 and ν_4 bands decreased by about 20 cm^{-1} , while there were small to negligible decreases for the ν_1 , ν_8 , and ν_9 bands. Polarization studies of the 1538 cm^{-1} band show that it consists of two bands: a polarized band at 1537 cm^{-1} and a depolarized band at 1541 cm^{-1} (Fig. 4). Based on the polarization studies, the first band was ascribed to ν_2 and the latter band to ν_{10} .

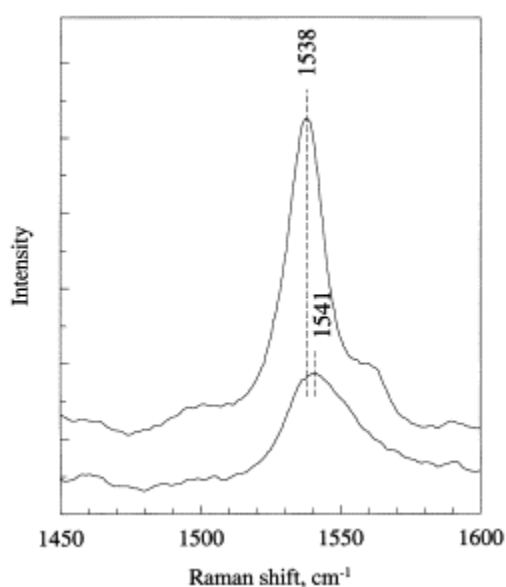


Fig. 4. Resonance Raman spectra of $1.0\text{ mM Fe}(\text{TPP})^{2-}$ in DMF with 0.1 M PNPCI : top spectrum, parallel polarization; lower spectrum, perpendicular polarization. Laser power, 28 mW ; excitation wavelength, 442 nm .

4. Discussion

The determining factor in the formation of a π -anion versus metal reduction product is the relative position of the e_g^* and the d_z^2 orbitals. This analysis can be complicated by the ability of the d_{π} -orbitals to back-bond with the e_g^* orbital. This would lead to electron flow back to the porphyrin and makes the analysis of π -anions more complex than π -cations [3]. Addition of an electron to the e_g^* orbitals will generate a π -anion radical, while reduction will be centered on the iron if the electron is added to the d_z^2 orbital.

Considerable empirical evidence has been collected relating the changes in the high-frequency modes with the porphyrin core size [22]. The core sizes of $\text{Fe}(\text{TPP})^-$ and $\text{Fe}(\text{TPP})^{2-}$ have been measured by Mashiko et al. [3] from their X-ray structures¹. They found that the $\text{Fe}-\text{N}_p$ distances of $\text{Fe}(\text{TPP})^-$ and $\text{Fe}(\text{TPP})^{2-}$ were 1.980 and 1.968 \AA , respectively. Both these distances are shorter than the $\text{Fe}^{\text{II}}(\text{TPP})(\text{L})_2$ distance of 2.000 \AA [23] and the expected values [3]. Using X-ray data, the data obtained by Parthasarathi et al. (open symbols) [22] and the data from this work (solid symbols), the relationship between core size and Raman shift for several bands are shown in Fig. 5. The changes observed in the $\text{Fe}(\text{TPP})^-$ spectrum are consistent with a decrease in the core size in going from

low-spin $\text{Fe}^{\text{II}}(\text{TPP})$ to low-spin $\text{Fe}^{\text{I}}(\text{TPP})^-$ [3]. For example, the ν_2 and ν_4 bands are consistent with the trend lines. While the ν_{10} Raman shift is significantly below the trend line, its frequency does increase when compared to the ferrous complex, which deviates significantly from the trend line due to back-bonding [22]. On the other hand, the Raman shifts for $\text{Fe}(\text{TPP})^{2-}$ do not correlate well with core size, with the observed shifts being in the opposite direction in most cases. Only the ν_4 mode shifts in the direction expected, but this mode is relatively insensitive to core-size changes. For the three other modes found, there were significant deviations (ν_2 , ν_3 and ν_{10} modes).

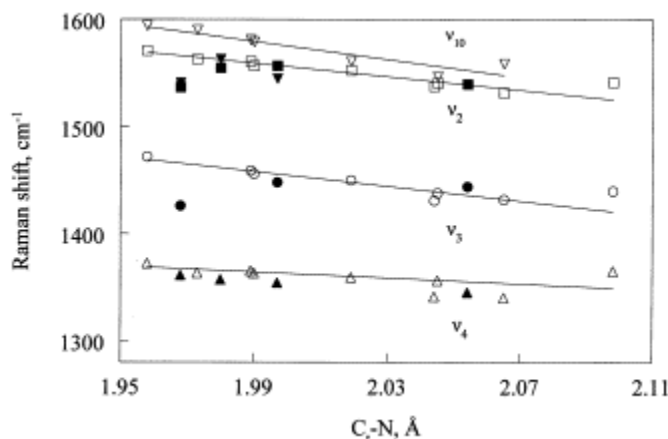


Fig. 5. Relationship between the high-frequency bands of $\text{M}(\text{TPP})$ and the X-ray crystallographic core size. Open symbols from Ref. [22]. Solid symbols: this work; from left to right: $\text{Fe}(\text{TPP})^{2-}$, $\text{Fe}(\text{TPP})^-$ and $\text{Fe}(\text{TPP})$ in DMF. The band for ν_3 was not observed for $\text{Fe}(\text{TPP})^-$.

The changes monitored in Fig. 5 were due to changes in the oxidation and/or spin state of the metal atom. Recent studies have shown that the formation of a π -anion can give rise to characteristic changes in the resonance Raman spectrum. These results are summarized in Table 2, along with changes in the same bands that have been observed for metal reduction. The formation of porphyrin π -anion radicals generally led to significant decreases in the ν_2 , ν_3 and ν_{10} bands, and small changes in the ν_4 band. On the other hand, changes due to metal reduction generally follow the trend lines derived by Parthasarathi et al. [22]. A comparison of the resonance Raman spectrum of $\text{Fe}(\text{TPP})^{2-}$ with $\text{Zn}(\text{TPP})^-$ and other π -anion radicals shows considerable agreement. For example, the ν_2 decreased by 18 cm^{-1} in the formation of $\text{Fe}(\text{TPP})^{2-}$, which compares with 16 cm^{-1} for the formation of $\text{Zn}(\text{TPP})^-$. Similarly, the ν_{10} band decreased by 22 and 19 cm^{-1} for the formation of $\text{Fe}(\text{TPP})^{2-}$ and $\text{Zn}(\text{TPP})^-$, respectively. Only small changes were observed in the ν_4 band in both cases. Another complex, $\text{Fe}(\text{TPP}(\text{CN})_4)^-$, which has considerable porphyrin π -anion character, was observed to have similar shifts [4]. Yamaguchi and Morishima [7] investigated this last complex in considerable detail using NMR. While it had considerable radical character, it was not a pure π -anion radical, and was formulated as a resonance form between an Fe(I) porphyrin and an Fe(II) porphyrin π -anion radical. The NMR of $\text{Fe}(\text{TPP})^{2-}$ was also not a pure π -anion radical [2], and so should be similarly characterized as a resonance hybrid. Back-bonding between the d_{π} -orbitals of the metal and the e_g porphyrin orbital probably accounts for the contraction of the core upon reduction. Comparisons with $\text{Fe}(\text{OEP})^{2-}$ show that the results are qualitatively and quantitatively different from $\text{Fe}(\text{TPP})^{2-}$. If the core size of $\text{Fe}(\text{OEP})$ also decreases with reduction as was observed for $\text{Fe}(\text{TPP})$, then the changes are consistent with the reduction of the metal.

Table 2. Shifts in structure sensitive resonance [Raman bands](#) of low valent metal [porphyrins](#) upon reduction

Oxidized/reduced species	$\Delta\nu_2$ (cm ⁻¹)	$\Delta\nu_4$ (cm ⁻¹)	$\Delta\nu_{10}$ (cm ⁻¹)	$\Delta\nu_3$ (cm ⁻¹)	Ref.
Formation of π -anions					
Zn(TPP)/Zn(TPP) ⁻	-16, -13	-1, -5	-19, -19		[9]
Zn(OEP)/Zn(OEP) ⁻	-12	-2	-26	-38	[12]
VO(OEP)/VO(OEP) ⁻	-11	-10	-31	-36	[12]
Fe(TPP(CN) ₄)(Is)/Fe(TPP(CN) ₄) ⁻	-18	-1			[4]
<i>Reduction of metal</i>					
Fe(TPP) ⁺ (Is)/Fe(TPP)(Is)	-4	-11	-36	-11	[22]
Fe(TPP)(hs)/Fe(TPP) ⁻ (Is)	+10	+12	-34	-2	this work
Fe(TPP)(Is)/Fe(TPP) ⁻ (Is)	-5	-2	+18		[4], [24]
Fe(OEP)(Im) ₂ /Fe(OEP) ⁻		+12	+11	-4	[5], [25]
<i>Iron(II) reduction</i>					
Fe(TPP) ⁻ /Fe(TPP) ²⁻	-18	+4	-22		this work
Fe(OEP) ⁻ /Fe(OEP) ²⁻		+17	+42	0	[5]

In addition to the direction of the Raman shifts, Hu et al. [12] also observed that π -anion radicals have significantly higher depolarization ratios for the ν_2 and ν_3 bands due to the Jahn–Teller effect. For Zn(OEP)⁻ (VO(OEP)⁻), the depolarization ratios were 0.24 (0.31) and 0.36 (0.32) for ν_2 and ν_3 , respectively. Similar results were obtained in this work where higher depolarization ratios (0.34 for ν_2 and 0.27 for ν_3) for Fe(TPP)²⁻ were also observed, which is consistent with an Fe^I(TPP⁻)²⁻ structure.

The resonance Raman spectra of Fe(TPP)⁻ and Fe(TPP)²⁻ in DMSO have been reported by Anxolabéhère et al. [6]. They avoided the use of DMF due to the instability of Fe(TPP)²⁻ in that solvent/electrolyte system, which we also observed. The Fe(TPP)²⁻ complex was stable in the presence of PNPCl salts, allowing us to obtain the resonance Raman spectrum in DMF. One would expect, though, that the resonance Raman spectra would be essentially the same in both solvents. In fact, significant differences were observed. In particular, the spectrum of Fe(TPP)²⁻ in DMSO (Fig. 2 in Ref. [6]) gave strong bands of roughly equal intensity at 1234, 1343, 1359, 1490 and 1545 cm⁻¹, and no band at 1537 cm⁻¹ (dominant band in our work). The visible spectra of Fe(P)⁻ and Fe(P)²⁻, though, were comparable to ours (their work utilized mostly pentafluorophenylporphyrin). One significant difference between our work is the excitation line (413.1 versus 442 nm). The 413.1 nm line is significantly off-resonance with the Fe(TPP)²⁻ absorption maximum (459 nm) and was in fact very near the minimum in the spectra. As a result, trace amounts of Fe^{II}(TPP) (and related species), which were not significant in the visible spectrum, will interfere with the resonance Raman spectra due to differences in their scattering ability. The resonance Raman spectrum of Fe^{II}(TPP)(OH)⁻, shown in Table 1, corresponds quite well with Fig. 2b (Fe(TPP)²⁻) in Ref. [6] (in parentheses): 1233 (1234), 1267 (1272), 1289 (1289), 1341 (1343), 1359 (1359), 1441 (1441), 1489 (1490), and 1545 (1545) cm⁻¹. Fig. 4c of Ref. [6], which was obtained at 457.9 nm (in resonance with Fe(TF₅TPP)²⁻), was similar to our work, but showed considerable interference due to the presence of Fe(TF₅TPP)⁻. Two bands were observed in the ν_4 region, 1344 and 1357 cm⁻¹. These bands are identical to the ν_4 bands found in work for Fe(TPP) and Fe(TPP)⁻, respectively (see Fig. 3). As was pointed out by Anxolabéhère et al. [6], photochemical decomposition of Fe(TPP)⁻ occurs quite readily, and a pure Fe(TPP)⁻ spectra can only be obtained with great difficulty. In fact, we were not able to obtain suitable resonance Raman spectra of low-valent iron porphyrins from a thin-layer spectroelectrochemical cell without significant photochemical reactions.

5. Conclusions

A stable $\text{Fe}(\text{TPP})^{2-}$ complex can be generated electrochemically if a non-alkylating supporting electrolyte is used, and this complex was examined spectroscopically. Resonance Raman data, obtained from electrochemically generated $\text{Fe}(\text{TPP})^{2-}$, indicated that $\text{Fe}(\text{TPP})^{2-}$ can be best characterized as an iron(I) porphyrin π -anion [12]. In addition, the Soret band for $\text{Fe}(\text{TPP})^{2-}$ appears to be sensitive to ion-pairing. Work is continuing in our laboratory to examine the infrared spectra of porphyrins and porphyrinones in order to determine the effect of macrocycle structure on the electronic structure of low valent iron porphyrins.

References

1. C.A Reed. *Adv. Chem. Ser.*, 201 (1982), pp. 333-356
2. G.N Sinyakov, A.M Shulga. *J. Mol. Struct.*, 295 (1993), p. 1
3. T Mashiko, C.A Reed, K.J Haller, W.R Scheidt. *Inorg. Chem.*, 23 (1984), p. 3192
4. R.J Donohoe, M Atamian, D.F Bocian. *J. Am. Chem. Soc.*, 109 (1987), p. 5593
5. J Teraoka, S Hashimoto, H Sugimoto, M Mori, T Kitagawa. *J. Am. Chem. Soc.*, 109 (1987), p. 180
6. E Anxolabéhère, G Chottard, D Lexa. *New J. Chem.*, 18 (1994), p. 889
7. K Yamaguchi, I Morishima. *Inorg. Chem.*, 31 (1992), p. 3216
8. D.L Hickman, A Shirazi, H.M Goff. *Inorg. Chem.*, 24 (1985), p. 563
9. R.A Reed, R Purrello, K Prendergast, T.G Spiro. *J. Phys. Chem.*, 95 (1991), p. 9720
10. H Yamaguchi, A Soeta, H Toeda, K Itoh. *J. Electroanal. Chem.*, 159 (1983), p. 347
11. M Atamian, R.J Donohoe, J.S Lindsey, D.F Bocian. *J. Phys. Chem.*, 93 (1989), p. 2236
12. S Hu, C.-Y Lin, M.E Blackwood Jr., A Mukherjee, T.G Spiro. *J. Phys. Chem.*, 99 (1995), p. 9694
13. X.Q Lin, K.M Kadish. *Anal. Chem.*, 57 (1985), p. 1498
14. R.S Czernuszewicz, K.A Macor. *J. Raman Spectrosc.*, 19 (1988), p. 553
15. C De Silva, K Czarnecki, M.D Ryan. *Inorg. Chim. Acta*, 226 (1994), p. 195
16. E.E Bancroft, J.S Sidwell, H.N Blount. *Anal. Chem.*, 53 (1981), p. 1390
17. K.M Kadish, R.K Rhodes. *Inorg. Chem.*, 22 (1983), p. 1090
18. C. De Silva, Ph.D. Thesis, Marquette University, 1997.
19. D Lexa, M Momenteau, J Mispelter. *Biochim. Biophys. Acta*, 338 (1974), p. 151
20. K.M Kadish, G Larson, D Lexa, M Momenteau. *J. Am. Chem. Soc.*, 97 (1975), p. 282
21. G.N Sinyakov, A.M Shul'ga. *Zh. Prikl. Spektrosk.*, 58 (1993), p. 126
22. N Parthasarathi, C Hansen, S Yamaguchi, T.G Spiro. *J. Am. Chem. Soc.*, 109 (1987), p. 3865
23. T Mashiko, C.A Reed, K.J Haller, M.E Kastner, W.R Scheidt. *J. Am. Chem. Soc.*, 103 (1981), p. 5758
24. H Oshio, T Ama, T Watanabe, J Kincaid, K Nakamoto. *Spectrochim. Acta, Part A*, 40 (1984), p. 863
25. T Kitagawa, H Ogoshi, E Watanabe, Z Yoshida. *J. Phys. Chem.*, 79 (1975), p. 2629

¹ The authors in Ref. [22] refer readers to Fig. 1 of Ref. [1] for the spectrum of $\text{Fe}(\text{TPP})^{2-}$. In fact, that figure and their data do not agree. The spectral data in Ref. [22] does agree with other reported values for $\text{Fe}(\text{TPP})^{2-}$.